

New layered oxysulfide SrFBiS₂

Hechang Lei, Kefeng Wang, Milinda Abeykoon, Emil S. Bozin, and C. Petrovic
*Condensed Matter Physics and Materials Science Department,
 Brookhaven National Laboratory, Upton, New York 11973, USA*
 (Dated: March 21, 2019)

We have synthesized a new layered BiS₂-based compound SrFBiS₂. This compound has similar structure to LaOBiS₂. It is built up by stacking up SrF layers and NaCl-type BiS₂ layers alternatively along the *c* axis. Electric transport measurement indicates that SrFBiS₂ is a semiconductor. Thermal transport measurement indicates that SrFBiS₂ has a small thermal conductivity and large Seebeck coefficient. First principle calculations are in agreement with experimental results and show that SrFBiS₂ is very similar to LaOBiS₂ which becomes superconductor with F doping. Therefore, SrFBiS₂ may be a parent compound of new superconductors.

PACS numbers: 74.10.+v, 74.70.Dd, 72.15.Jf, 71.20.Nr

I. INTRODUCTION

Low-dimensional superconductors with layered structure have been extensively studied and still attract much interest due to their exotic superconducting properties and mechanism when compared to conventional BCS superconductors. The examples include high T_c cuprates,¹ Sr₂RuO₄,² Na_xCoO₂·H₂O,³ and iron-based superconductors.⁴ The discovery of LnOFePn (Ln = rare earth elements, Pn = P, As) in particular revitalises the study of layered compounds with mixed anions, paving a way to materials with novel physical properties. For example, Ln₂O₂TM₂OCh₂ (TM = transition metals, Ch = S, Se) show strong electron-electron interactions and Mott insulating state on the two dimensional (2D) frustrated antiferromagnetic (AFM) checkerboard spin-lattice.^{5–9} Very recently, bulk superconductivity was found in BiS₂-type layered compounds with mixed anions: Bi₄O₄S₃ and Ln(O,F)BiS₂.^{10–12} Experimental and theoretical studies indicate that these materials exhibit multiband behaviors with dominant electron carriers originating from the Bi $6p_x$ and $6p_y$ bands in the normal state.^{13–16} On the other hand, compounds with mixed anions exhibit remarkable flexibility of structure. Different two-dimensional (2D) building blocks, such as [LnO]⁺, [AEF]⁺ (AE = Ca, Sr, Ba), [Ti₂OPn₂]^{2–}, [FePn][–], and [TM₂OCh₂]^{2–}, can sometimes be integrated to form new materials.^{4,17–21} Individual building blocks often keep their structural and electronic properties after being combined together.¹⁹

In this work, we report the discovery of a new BiS₂-based layered compound SrFBiS₂. It contains NaCl-type BiS₂ layer and shows semiconducting behavior with relatively large thermopower. Theoretical calculation indicates that this compound is very similar to LnOBiS₂.

II. EXPERIMENT

SrFBiS₂ polycrystals were synthesized by a two-step solids state reaction. First, Bi₂S₃ was prereacted by reacting Bi needles (purity 99.99%, Alfa Aesar) with sulfur

flakes (purity 99.99%, Aldrich) in an evacuated quartz tube at 600 °C for 10 h. Then Bi₂S₃ was mixed with stoichiometric SrF₂ (purity 99%, Alfa Aesar) and SrS (purity 99.9%, Alfa Aesar) and intimately ground together using an agate pestle and mortar. The ground powder was pressed into pellets, loaded in an alumina crucible and then sealed in quartz tubes with Ar under the pressure of 0.15 atmosphere. The quartz tubes were heated up to 600 °C in 10 h and kept at 600 °C for another 10 h.

Phase identity and purity were confirmed by powder X-ray diffraction carried out by a Rigaku Miniflex X-ray machine with Cu K_α radiation ($\lambda = 1.5418$ Å). Structural refinements of powder SrFBiS₂ sample was carried out by using Rietica software.²² Synchrotron X-ray experiment was conducted at 300 K on X17A beamline of the National Synchrotron Light Source (NSLS) at Brookhaven National Laboratory (BNL). The setup utilized X-ray beam 0.5 mm × 0.5 mm in size and 0.1839 Å ($E = 67.4959$ keV), conditioned by two-axis focusing with one-bounce sagittally-bent Laue crystal monochromator, and Perkin-Elmer image plate detector mounted perpendicular to the primary beam path. Finely pulverized sample packed in cylindrical polyimide capillary 1mm in diameter was placed 204 mm away from the detector. Multiple scans were performed to a total exposure time of 120 s. The 2D diffraction data were integrated and converted to intensity versus 2θ using the software FIT2D.²³ The intensity data were corrected and normalized and converted to atomic pair distribution function (PDF), $G(r)$, using the program PDFgetX2.²⁴

The samples were cut into rectangular bar and thin Pt wires were attached for four probe resistivity measurements. Electrical and thermal transport measurements were carried out in PPMS-9.

First principle electronic structure calculation were performed using experimental crystallographic parameters within the full-potential linearized augmented plane wave (LAPW) method²⁵ implemented in WIEN2k package.²⁶ The general gradient approximation (GGA) of Perdew *et al.*,²⁷ was used for exchange-correlation potential. The LAPW sphere radius were set to 2.5 Bohr

TABLE I. Crystallographic Data for SrFBiS₂ obtained from synchrotron powder XRD.

Chemical Formula		SrFBiS ₂		
Formula Mass (g/mol)		379.73		
Crystal System		Tetragonal		
Space Group		P4/nmm (No. 129)		
<i>a</i> (Å)		4.079(2)		
<i>c</i> (Å)		13.814(5)		
<i>V</i> (Å ³)		229.8(3)		
<i>Z</i>		2		
Density (g/cm ³)		5.51		
Atom site	x	y	z	
Sr 2c	1/4	1/4	0.1025(2)	
F 2a	3/4	1/4	0	
Bi 2c	1/4	1/4	0.6286(5)	
S1 2c	1/4	1/4	0.3793(25)	
S2 2c	1/4	1/4	0.8112(15)	

for all atoms, and the converged basis corresponding to $R_{min}k_{max} = 7$ with additional local orbital were used where R_{min} is the minimum LAPW sphere radius and k_{max} is the plane wave cutoff.

III. RESULTS AND DISCUSSION

Fig. 1(a) shows the powder XRD pattern of SrFBiS₂ measured by Rigaku Miniflex. Almost all of reflections can be indexed using the P4/nmm space group. The refined lattice parameters of SrFBiS₂ are $a = 4.077(2)$ Å and $c = 13.800(2)$ Å, both of which are close to the values of LaOBiS₂.¹¹ The reflection located at about 28.4° originates from the Bi₂S₃ impurity. The PDF structural analysis was carried out using the program PDFgui.²⁸ The SrFBiS₂ data are explained well within the model having P4/nmm symmetry with $a = 4.079(2)$ Å and $c = 13.814(5)$ Å. It is consistent with the fitting results obtained from Miniflex. The final fit is shown in Fig. 1(b), and the results are summarized in Table 1. In addition to the principal phase, the sample is found to have ~ 12(1) atomic % of Bi₂S₃ impurity with Pnma symmetry, which is also observed in Fig. 1(a). Structure of SrFBiS₂ is similar to LaOBiS₂, which is built up by stacking the rock-salt-type BiS₂ layer and fluorite-type SrF layer alternatively along the *c* axis as shown Fig. 1(c).

As shown in Fig. 2, polycrystalline resistivity $\rho(T)$ of SrFBiS₂ polycrystalline shows a semiconducting behavior in the measured temperature region. It should be noted that Bi₂S₃ polycrystal shows metallic behavior because of sulfur deficiency.²⁹ The impurity may have some minor influence on the absolute value of resistivity, but the semiconducting behavior should be intrinsic. Neglecting the grain boundary contribution, the room-temperature resistivity $\rho(300$ K) is about 0.5 Ω·cm. Using the ther-

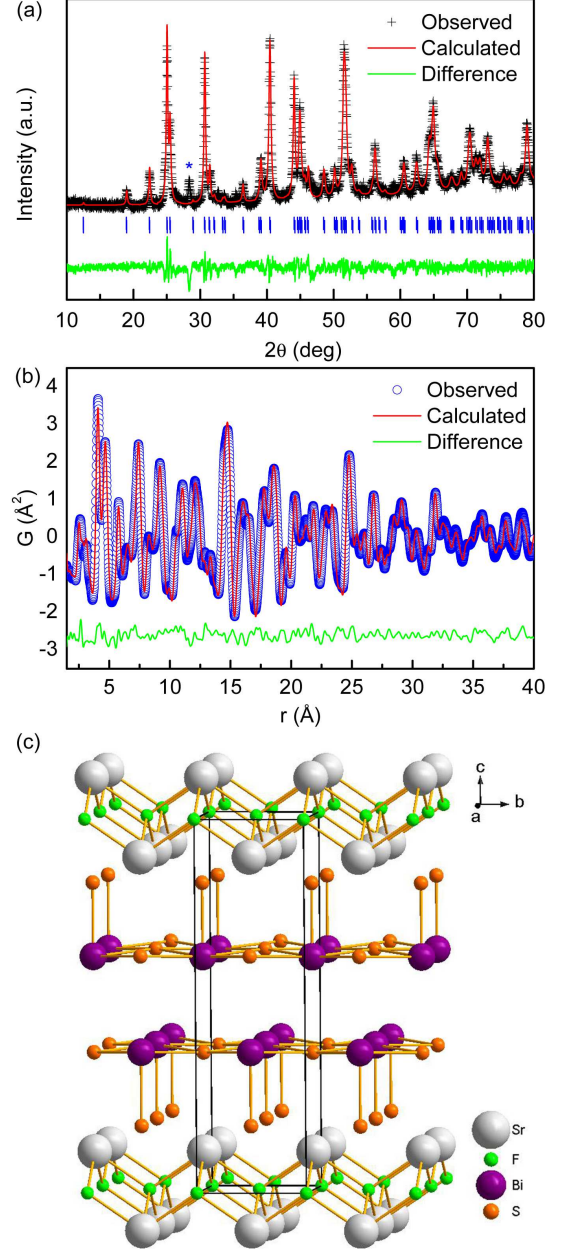


FIG. 1. (a) Powder XRD pattern of SrFBiS₂. The asterisks mark the peaks from Bi₂S₃. (b) Synchrotron PDF refinement results taken at room temperature. (c) Crystal structure of SrFBiS₂. The biggest white, big purple, medium orange, and small green balls represent Sr, Bi, S, and F ions, respectively.

mal activation model $\rho_{ab}(T) = \rho_0 \exp(E_a/k_B T)$ (ρ_0 is a prefactor, E_a thermal activated energy and k_B the Boltzmann's constant) to fit the $\rho(T)$ at high temperature (75 K - 300 K) (inset of Fig. 2), we obtain $E_a = 31.8(3)$ meV. The semiconductor behavior is consistent with theoretical calculation result shown below. On the other hand, theoretical calculations have indicated that

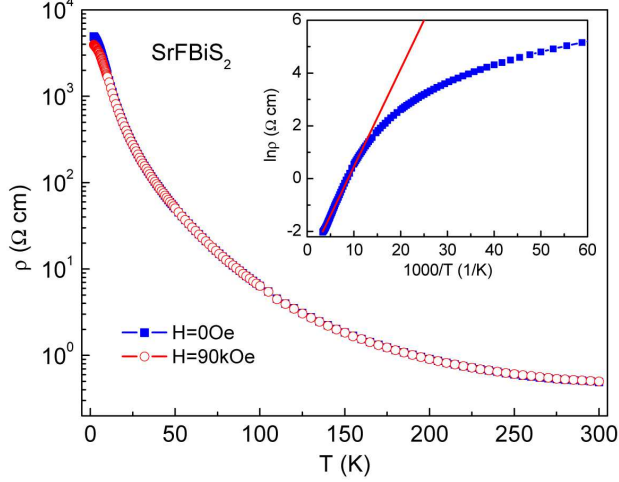


FIG. 2. Temperature dependence of the resistivity $\rho(T)$ of the SrFBiS₂ at $H = 0$ (closed blue square) and 90 kOe (open red circle). Inset shows the fitted result using thermal activation model for $\rho(T)$ at zero field where the red line is the fitting curve.

undoped LaOBiS₂ is also a semiconductor, but with no experimental verification so far.^{13,30} Present results suggest that LaOBiS₂ should also exhibit semiconductor behavior in $\rho(T)$ curve because the replacement of LaO by SrF should not change the band structure and thus physical properties much, similar to the relation between SrFeAs and LaOFeAs.^{18,31} Moreover, the resistivity of LaO_{0.5}F_{0.5}BiS₂ in the normal state shows semiconducting behavior,^{11,30} which also suggests that LaOBiS₂ should be a semiconductor. Note that the semiconducting $\rho(T)$ in LaOBiS₂ and SrFBiS₂ are different from those in parent compounds of iron pnictide superconductors. The latter show metallic behaviors at high temperature and semiconducting-like upturn in resistivity curve related to the spin density wave (SDW) transition. There is no significant magnetoresistance in SrFBiS₂ up to 90 kOe magnetic field.

The temperature dependences of the thermal conductivity $\kappa(T)$ and thermoelectric power (TEP) $S(T)$ for SrFBiS₂ in zero field between 2 and 350 K are shown in Fig. 3. The electronic thermal conductivity $\kappa_e(T)$ estimated from the Wiedemann-Franz law using a value for the Lorenz number of 2.44×10^{-8} W Ω /K² was less than 5×10^{-6} of $\kappa(T)$. Therefore, lattice thermal conductivity dominates $\kappa_L(T)$ which exhibits a peak at around 60 K (Fig. 1(a)). The peak in $\kappa(T)$ commonly arises since different phonon scattering processes usually dominate in different temperature ranges. Umklapp scattering dominates at high temperatures, while boundary and point-defect scattering dominate at low and intermediate temperatures, respectively.³² On the other hand, the $\kappa(T)$ of SrFBiS₂ shows similar behavior to Bi₄O₄S₃ but with different peak position and absolute value.¹⁶ For TEP $S(T)$

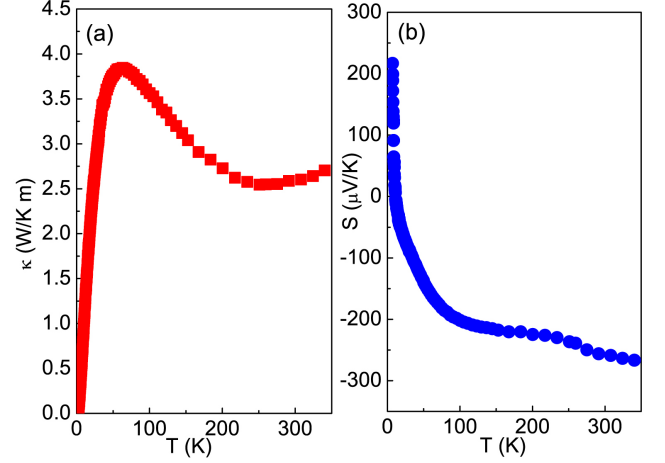


FIG. 3. Temperature dependence of (a) thermal conductivity and (b) thermoelectric power for SrFBiS₂ under zero magnetic field within a temperature range from 2 to 340 K.

of SrFBiS₂, there is a reversal in sign at about 11 K, i.e., hole-like carrier changes into electron-like carrier which is dominant at room temperature. According to two band model, $S = |S_h|\sigma_h - |S_e|\sigma_e/(\sigma_e + \sigma_h)$.¹⁶ If we assume that S_h and S_e are temperature independent, it suggests that electron and hole conductivities change dramatically with temperature: at low temperature, $\sigma_h > \sigma_e$ whereas $\sigma_e > \sigma_h$ above 11 K. Hole-like carrier may originate from defect induced p-type doping. With increasing temperature, electron-like carrier due to intrinsic band excitation increase significantly, finally leading to $\sigma_e > \sigma_h$ and a sign change in $S(T)$. Similar behavior was observed in LaOZnP and p-type Si.^{16,33} Even though the $S(T)$ in SrFBiS₂ is significant and not much smaller than in classics thermoelectric materials,³⁵ its low electrical conductivity makes its figure of merit ZT ($ZT = \sigma S^2 T / \kappa$) extremely small.

First principle calculations (Fig. 4) confirm that SrFBiS₂ is a semiconductor with a direct band gap of 0.8 eV located at X point. This is similar to LaOBiS₂ where the energy gap was found to be 0.82 eV.³⁶ The calculation confirms the results of transport measurement. Similar to LaOBiS₂,^{13,36} both S 3p and Bi 6p states are located around the Fermi level (-2.0 to 2.0 eV) in SrFBiS₂. Thus there is a strong hybridization between S 3p and Bi 6p states. The absence of dispersion along $\Gamma - Z$ line suggests quasi two dimensional character of the band structure in SrFBiS₂ (Fig. 4(b)). In LaOBiS₂, F doping results in metallic states and superconductivity at low temperature. Main influence of F substitution is a carrier doping that shifts the Fermi level and has only minor effect on the lowest conduction band. Due to similarity between SrFBiS₂ and LaOBiS₂, new superconductors could be obtained by chemical substitution.

IV. CONCLUSION

In summary, we report a discovery of a new layered iron oxychalcogenide SrFBiS_2 . It contains NaCl-type BiS_2 layer similar to $\text{Bi}_4\text{O}_4\text{S}_3$ and $\text{Ln}(\text{O},\text{F})\text{BiS}_2$ superconductors. SrFBiS_2 polycrystals shows semiconducting behavior between 2 K and 300 K. We observe rather small thermal conductivity and large TEP with sign reversal at low temperature. Theoretical calculation confirms the semiconducting behavior and indicates similar DOS and band structure to undoped LaOBiS_2 . Because of the similarity between SrFBiS_2 and the parent compound of BiS_2 -based superconductors, it is of interest to investigate the doping effects on physical properties of SrFBiS_2 . It could pave a way to new members in this emerging family of BiS_2 -based superconductors.

V. ACKNOWLEDGEMENTS

Work at Brookhaven is supported by the U.S. DOE under Contract No. DE-AC02-98CH10886 and in part by the Center for Emergent Superconductivity, an Energy Frontier Research Center funded by the U.S. DOE, Office for Basic Energy Science (H. L. and C. P.). This work benefited from usage of X17A beamline of the National Synchrotron Light Source at Brookhaven National Laboratory.

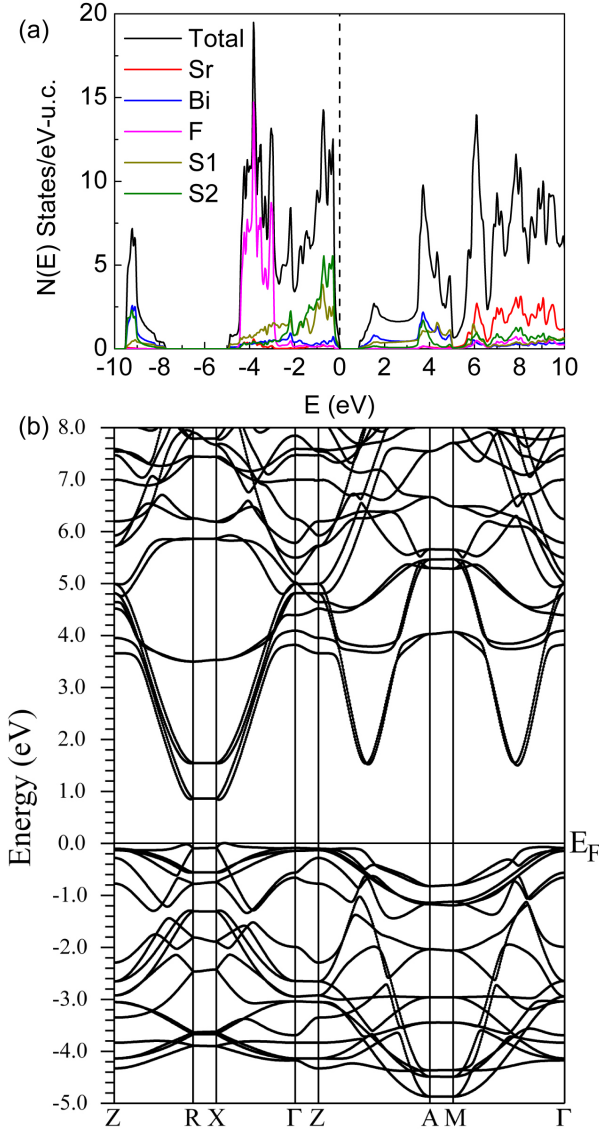


FIG. 4. (a) Total and atom resolved density of states and (b) band structure of SrFBiS_2 .

- ¹ J. G. Bednorz and K. A. Muller, *Z. Physik B* **64**, 189 (1986).
- ² Y. Maeno, H. Hashimoto, K. Yoshida, S. Nishizaki, T. Fujita, J. G. Bednorz, and F. Lichtenberg, *Nature* **372**, 532 (1994).
- ³ K. Takada, H. Sakurai, E. Takayama-Muromachi, F. Izumi, R. A. Dilanian, and T. Sasaki, *Nature* **422**, 53 (2003).
- ⁴ Y. Kamihara, T. Watanabe, M. Hirano, and H. Hosono, *J. Am. Chem. Soc.* **130**, 3296 (2008).
- ⁵ J. M. Mayer, L. F. Schneemeyer, T. Siegrist, J. V. Waszczak and B. Van Dover, *Angew. Chem., Int. Ed. Engl.* **31**, 1645 (1992).
- ⁶ C. Wang, M. Q. Tan, C. M. Feng, Z. F. Ma, S. Jiang, Z. A. Xu, G. H. Cao, K. Matsubayashi and Y. Uwatoko, *J. Am. Chem. Soc.* **132**, 7069 (2010).
- ⁷ J.-X. Zhu, R. Yu, H. Wang, L. L. Zhao, M. D. Jones, J. Dai, E. Abrahams, E. Morosan, M. Fang and Q. Si, *Phys. Rev. Lett.* **104**, 216405 (2010).
- ⁸ N. Ni, E. Climent-Pascual, S. Jia, Q. Huang and R. J. Cava, *Phys. Rev. B* **82**, 214419 (2010).
- ⁹ D. G. Free, N. D. Withers, P. J. Hickey and J. O. Evans, *Chem. Mater.* **23**, 1625 (2011).
- ¹⁰ Y. Mizuguchi, H. Fujihisa, Y. Gotoh, K. Suzuki, H. Usui, K. Kuroki, S. Demura, Y. Takano, H. Izawa, O. Miura, arXiv 1207.3145.

- ¹¹ Y. Mizuguchi, S. Demura, K. Deguchi, Y. Takano, H. Fujihisa, Y. Gotoh, H. Izawa, O. Miura, arXiv 1207.3558.
- ¹² S. Demura, Y. Mizuguchi, K. Deguchi, H. Okazaki, H. Hara, T. Watanabe, S. J. Denholme, M. Fujioka, T. Ozaki, H. Fujihisa, Y. Gotoh, O. Miura, T. Yamaguchi, H. Takeya, and Y. Takano, arXiv 1207.5248.
- ¹³ H. Usui, K. Suzuki, K. Kuroki, arXiv 1207.3888.
- ¹⁴ S. Li, H. Yang, J. Tao, X. Ding, and H.-H. Wen, arXiv 1207.4955.
- ¹⁵ S. K. Singh, A. Kumar, B. Gahtori, Shruti, G. Sharma, S. Patnaik, and V. P. S. Awana, arXiv 1207.5428.
- ¹⁶ S. G. Tan, L. J. Li, Y. Liu, P. Tong, B. C. Zhao, W. J. Lu, Y. P. Sun, arXiv 1207.5395.
- ¹⁷ S. Matsuishi, Y. Inoue, T. Nomura, H. Yanagi, M. Hirano, and H. Hosono, *J. Am. Chem. Soc.* **130**, 14428 (2008).
- ¹⁸ F. Han, X. Y. Zhu, G. Mu, P. Cheng, and H.-H. Wen, *Phys. Rev. B* **78**, 180503 (2008).
- ¹⁹ H. Kabbour, L. Cario, and F. Boucher, *J. Mater. Chem.* **15**, 3525 (2005).
- ²⁰ R. H. Liu, J. S. Zhang, P. Cheng, X. G. Luo, J. J. Ying, Y. J. Yan, M. Zhang, A. F. Wang, Z. J. Xiang, G. J. Ye and X. H. Chen, *Phys. Rev. B* **83**, 174450 (2011).
- ²¹ R. H. Liu, Y. A. Song, Q. J. Li, J. J. Ying, Y. J. Yan, Y. He, and X. H. Chen, *Chem. Mater.* **22**, 1503 (2010).
- ²² Hunter B. (1998) "Rietica - A visual Rietveld program", International Union of Crystallography Commission on Powder Diffraction Newsletter No. 20, (Summer) <http://www.rietica.org>
- ²³ A. P. Hammersley, S.O. Svenson, M. Hanfland, and D. Hauserman, *High Press. Res.* **14**, 235 (1996).
- ²⁴ X. Qiu, J. W. Thompson, and S. J. L. Billinge, *J. Appl. Crystallogr.* **37**, 678 (2004).
- ²⁵ M. Weinert, E. Wimmer, and A. J. Freeman, *Phys. Rev. B* **26**, 4571 (1982).
- ²⁶ P. Blaha, K. Schwarz, G. K. H. Madsen, D. Kvasnicka and J. Luitz, WIEN2k, An Augmented Plane Wave + Local Orbitals Program for Calculating Crystal Properties (Karlheinz Schwarz, Techn. Universitat Wien, Austria), 2001. ISBN 3-9501031-1-2
- ²⁷ J. P. Perdew, K. Burke and M. Ernzerhof, *Phys. Rev. Lett.* **77**, 3865 (1996).
- ²⁸ C. L. Farrow, P. Juhas, J. W. Liu, D. Bryndin, E. S. Bozin, J. Bloch, Th. Proffen, and S. J. L. Billinge, *J. Phys.: Condens. Mater.* **19**, 335219 (2007).
- ²⁹ B. Chen, C. Uher, L. Iordanidis, and M. G. Kanatzidis, *Chem. Mater.* **9**, 1655 (1997).
- ³⁰ V. P. S. Awana, A. Kumar, R. Jha, S. Kumar, J. Kumar, and A. Pal, arXiv 1207.6845.
- ³¹ J. Dong, H. J. Zhang, G. Xu, Z. Li, G. Li, W. Z. Hu, D. Wu, G. F. Chen, X. Dai, J. L. Luo, Z. Fang, and N. L. Wang, *EPL* **83**, 27006 (2008).
- ³² J. Yang, D. T. Morelli, G. P. Meisner, W. Chen, J. S. Dyck, and C. Uher, *Phys. Rev. B* **65**, 094115 (2002).
- ³³ K. Seeger, in *Semiconductor Physics: An Introduction*, Springer-Verlag, Berlin (2004).
- ³⁴ K. Kayanuma, H. Hiramatsu, M. Hirano, R. Kawamura, H. Yanagi, T. Kamiya, H. Hosono, *Phys. Rev. B* **76**, 195325 (2007).
- ³⁵ D. M. Rowe, in *Thermoelectrics Handbook: Macro to Nano*, Taylor & Francis, London (2006).
- ³⁶ X. Wan, H.-C. Ding, S. Y. Savrasov, and C.-G. Duan, arXiv 1207.5395.